Some Radiofrequency-Millimeterwave-Double Resonance Experiments, Partly with HFS-levels

M. Suzuki *, A. Guarnieri, and H. Dreizler

Abteilung Chemische Physik im Institut für Physikalische Chemie der Universität Kiel

(Z. Naturforsch. **31 a**, 1181–1189 [1976]; received July 3, 1976)

We report double resonance experiments with a broad range of pump frequencies up to 3.9 GHz and millimeter wave signal frequencies up to 160 GHz. It is demonstrated by the HFS of a rotational band head that these experiments provide a useful tool for analysing complex spectra in the range below 4 GHz.

In this paper we report double resonance experiments with pump frequencies from 1 MHz to 3,900 MHz (RF) and signal frequencies in the millimeter wave region up to 160 GHz (MMW). With this work we continued our efforts in investigating and applying double resonance techniques in microwave spectroscopy [1–8].

Although microwave-microwave (MW-MW) [9–13], microwave-millimeterwave (MW-MMW) [14] and radiofrequency-microwave (RF-MW) [15–17] double resonance has widely been used, no experiments have been reported to our knowledge using such a broad range of RF for the pump and MMW for the signal frequencies. Some examples will be given. One will be the application to the analysis of the HFS of a rotational band head by pumping HFS transitions.

Experimental

The main features of the apparatus are given in Figure 1. The most critical part is the absorption cell (1) **, 1.50 m long, made of X-band brass waveguide. It was tested to transmit RF to 4.5 GHz by a crystal detector 1 N 23 (2) above and an oscilloscope (3) (Tektronix 7904 + 7A19) below 1 GHz. We think that the transmission is a "coaxial"-type mode with a septum (4) like a stark septum as inner and the waveguide as the outer conductor. The ends of the septum were tapered as drawn in Figure 1. The vacuum tight connectors (5) are as given in Fig. 1 of Reference [6].

Reprint requests to Prof. Dr. A. Guarnieri, Institut für Physikalische Chemie der Universität Kiel, Olshausenstraße 40–60, *D-2300 Kiel.*

* Present adress: Dr. M. Suzuki, Dept. of Electronic Engineering, Tokyo College of Photography, 1583 Iyama, Atsugi-Shi, *Kanagawa, 243-02*, Japan.

** Numbers in brackets refer to Figure 1.

This construction reduces missmatch of the absorption cell and the RF- and MMW-generators. There is still a missmatch at the point, where the connecting wire is introduced in the waveguide.

For millimeter waves the cell was tested up to 220 GHz.

The millimeter waves were produced by a modified Gordy-Type multiplier (6) with Phosphor diffused Silicon cristals driven by a klystron (7) (OKI 30V12, 35V12, 40V12) in an oil bath. At fixed frequencies the klystron can be phase stabilised with a frequency standard (10) (Schomandl ND 800 M) and a synkriminator (11) (Schomandl FDS30).

In the free sweep mode markers are produced by the frequency standard (10) and narrow band receiver (14) (Collins Radio R3 90/URR).

The RF is taken from an oscillator (15) (Hewlett-Packard 3200 B; 10 to 520 MHz) controlled by a counter (16) (Hewlett-Packard 5303 B + 5300 A). The on-off modulation was made by a ring-mixer (17) (Mini-Circuits Lab ZAY 2) fed with continous wave RF and a 2 to 50 kHz square wave from a pulse generator (18) (Amritsu MG 412 A). The modulated RF was amplified, if necessary (19) by an amplifier (EIN 310 L, Hughes 46111 H).

RF-frequencies above 2.3 GHz were supplied by an oscillator (Rohde & Schwarz SLRC 0.5 – 3 Watts in 50 Ω), which can be amplitude modulated. The oscillator was phase stabilised by a frequency standard (21) (Schomandl FD3), a mixer (22) (Rohde & Schwarz XME) and a synkriminator (23) (Rohde & Schwarz XKG). A free sweep was made by a motor drive (24). In this mode of operation markers can be produced by the frequency standard (21) and the receiver (14). The detection system was built by a modified Gordy-Type detector (25), followed by a preamplifier (26) (PAR 113) a phase sensitive detector (27) (Tekelec TE 9000) and a recorder (28).

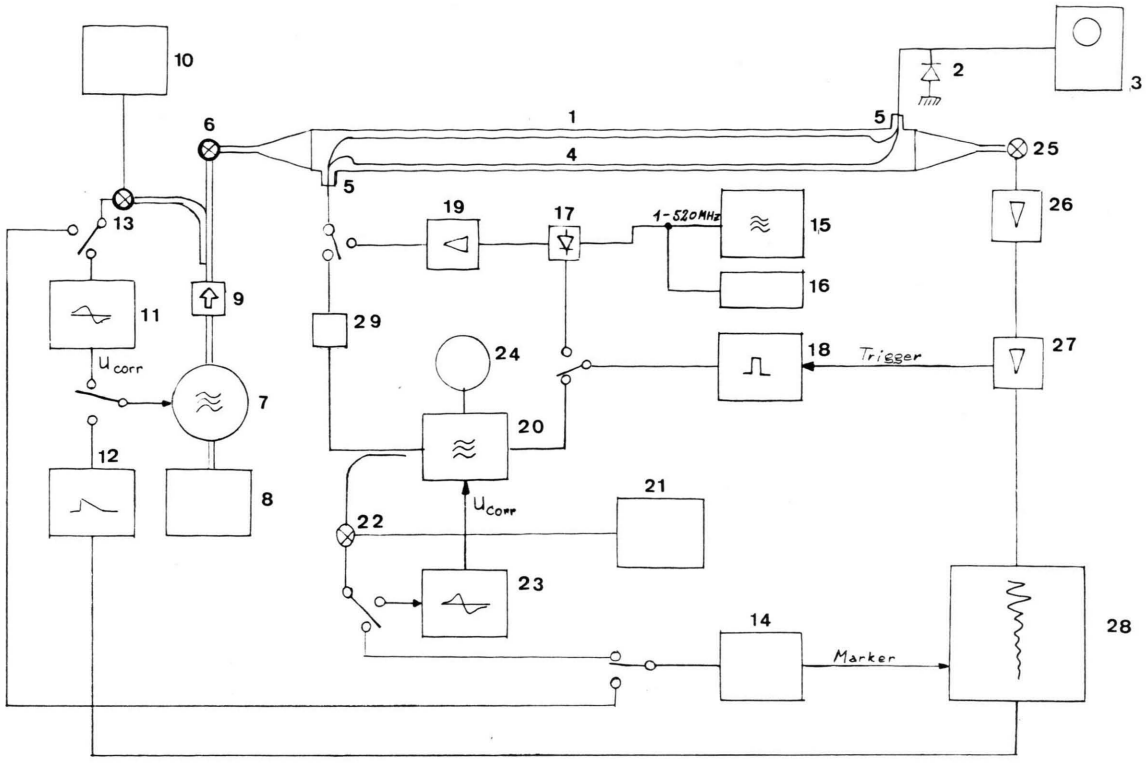

Fig. 1. RF-MMW-Double Resonance.

Spectrometer: 1 Absorptions cell, X-band, 1.5 m. 2 Crystal detector, 1N23. 3 Oscilloscope, Tektronix 7904+7A19. 4 Septum with tapered ends. 5 Vacuum tight connectors. 6 Modified Gordy type multiplier. 7 Klystron, OKI 30V12, 35V12, 40V12. 8 Klystron power supply. 9 Uniline. 10 Frequency standard, Schomandl ND800M. 11 Synkriminator, Schomandl FDS30. 12 Sweep generator. 13. Waveguide mixer. 14 Allwave narrowband receiver Collins Radio 390/URR. 15 Oscillator 10–520 MHz 200–25 mW Hewlett-Packard 3200 B. 16 Counter Hewlett Packard 5303 B–5300 A. 17 Ring mixer Mini Circuits Lab ZAY 2. 18 Pulse generator Amritsu MG 412 A. 19 Broadband amplifier (EIN 310 L, Hughes 46111H). 20 Oscillator 2.3–7 GHz 0.5–3 W Rohde & Schwarz SLRC. 21 Frequency standard, Schomandl FD 3. 22 Coaxial mixer, Rohde & Scharz XME. 23 Synkrimminator, Rohde & Schwarz XKG. 24 Motor drive. 25 Modified Gordy-type detector. 26 Preamplifier PAR 113. 27 Phase sensitive detector Tekelec TE 9000. 28 Recorder. 29 RF-Tuner.

The RF-MMW-spectrometer was used in two operational modes.

I) Pump frequency fixed and signal frequency swept,

II) Pump frequency swept and signal frequency fixed.

Figure 2 demonstrates mode I. The pump frequency was set to 3178. 92 MHz to pump the $J_{K_-K_+} \rightarrow J'_{K'_-K'_+} = 10_{2,9} \rightarrow 10_{2,8}$ $F = 17/2,\ 23/2 \rightarrow F' = 17/2,\ 23/2$ transition of $CD_3O^{35}Cl$, the signal frequency was swept around 105,265.55 MHz. The line showes the usual pattern of phase sensitive detection. The energy levels are given in Figure 3.

The mode II is presented also in Figure 3. Here the pump frequency ν_p was swept, the signal frequency ν_s was used as a monitor gaining sensitivity by $(\nu_s/\nu_p)^2 \approx 10^3$. So the intensity problems in the frequency range below 4000 MHz may be overcome

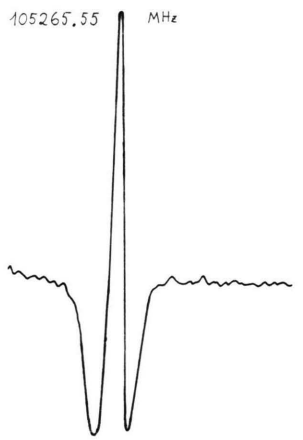

Fig. 2. $9_{27} \rightarrow 10_{28}$, $\Delta F = 1$ transition of $CD_3O^{35}Cl$ at 105 265.42 MHz, $10_{29} \rightarrow 10_{28}$ pumped with 3178.92 MHz, 1 W and 2.7 kHz modulation frequency of the pump. Operational mode I. For level diagram see Figure 3.

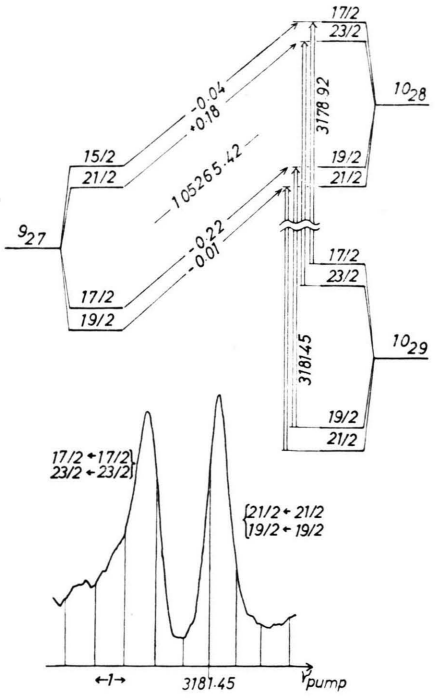

Fig. 3. Rotational energy level diagram for the transition $9_{27} \rightarrow 10_{28}$ of Fig. 2 and HFS of the $10_{29} \rightarrow 10_{28}$, $\Delta F=0$ transition (MHz) of $CD_3O^{35}Cl$ recorded with operational mode II. Line peaks are shifted by 0.25 MHz to higher frequencies due to the time constant of 1 sec. Modulation frequency 2.7 kHz.

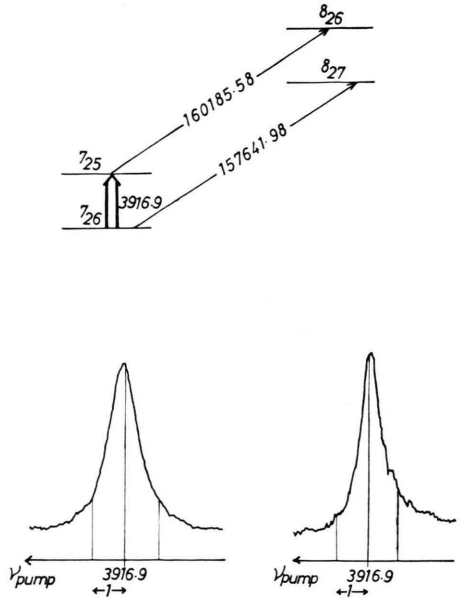

Fig. 4. Rotational energy level diagram and observed $7_{26} \rightarrow 7_{25}$ transition (MHz) of $CH_2{=}CHF$. $7_{25} \rightarrow 8_{26}$ and $7_{26} \rightarrow 8_{27}$ was used as monitor. Operational mode II. 2.7 kHz modulation frequency time constant 0.3 sec.

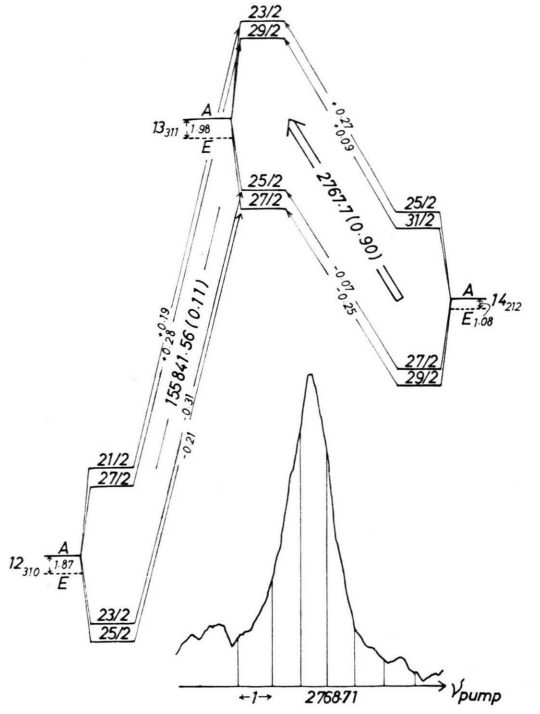

Fig. 5. Rotational energy level diagram and observed $13_{3,11} \rightarrow 14_{2,12}$ transition (MHz) of CH_3OCl. $12_{3,10} \rightarrow 13_{3,11}$ was used as monitor. Operational mode II. Values in brackets are torsional A−E splittings calculated with reduced barrier height $s=74.5$. Line peak is shifted by 0.3 MHz to higher frequency due to a time constant of 1 sec. Modulation frequency 2.7 kHz.

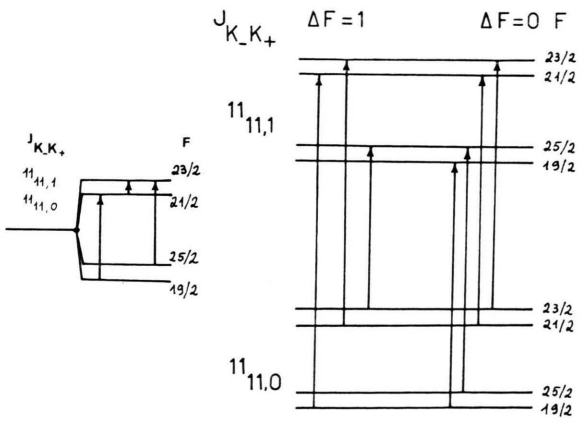

Fig. 6. Transitions within HFS levels of a near prolate top. At the right hand side the J_{K-K+} $11_{11,1}$ and $11_{11,0}$ levels are given in an expanded scale. $\Delta F=+1$ and 0, $\Delta J=0$, $\Delta K_-=0$, $\Delta K_+=1$ transitions are given by arrows, $\Delta F=-1$ transitions are not drawn. They cannot be distinguished from $\Delta F=+1$ when the J_{K-K+} levels coincide (left hand side).

in special cases. The HFS is clearly resolved. As shown in Table 1 the observed pattern agrees with the calculated one using molecular constants reported in [18].

In Fig. 4 it was checked, that the pump frequency is independent of the signal (monitor) frequency. In both cases setting $\nu_s = 157{,}641.98$ MHz for $7_{26} \rightarrow 8_{27}$ or $\nu_s = 160{,}185.58$ MHz for $7_{25} \rightarrow 8_{26}$ the pump frequency resulted as $\nu_p = 3916.9$ MHz for $7_{26} \rightarrow 7_{25}$ for $CH_2 = CHF$.

The recording of Fig. 5 was made in attempting to resolve the torsional fine structure of CH_3OCl, which was estimated with the reduced barrier height $s = 74.5$ to be approximately 0.9 MHz for the $13_{3,11} \rightarrow 14_{2,12}$ transition at $\nu_p = 2767$ MHz. As can be seen the fine structure was not resolved, presumably as the HFS fine structure interferes with the torsional fine structure.

As a final application we present a HFS-analysis of the band head of the $CH_3O^{35}Cl$ $J = 11 \rightarrow 12$

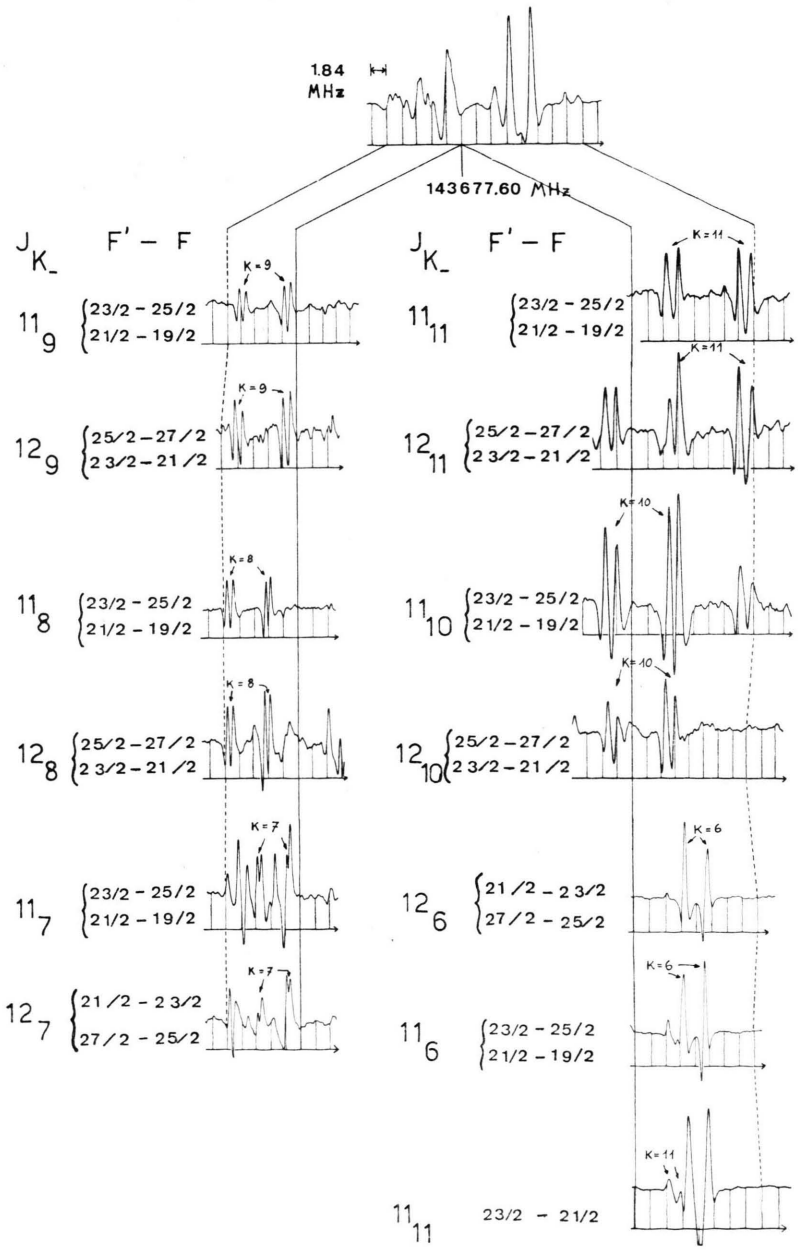

Figs. 7 a–h from top to bottom. r right, l left. a gives the contour of the $J = 11 \rightarrow 12$, $\Delta K_- = 0$ band head of $CH_3O^{35}Cl$ recorded by 1.5 kHz Stark-modulation with approx. 22 V/cm. Marker distance 1.84 MHz. b–h give details of the band head worked out with double resonance operational mode I. Pump transitions and frequencies are listed in Table 2. The observed lines have been used for the double resonance plot Fig. 9 and are listed in Table 3.

$J_{K_-K_+} \rightarrow J'_{K_-K'_+}$	$F \rightarrow F'$	ν_{obs}	ν^0_{obs}	ν_{calc}	$\delta\nu_{obs}$	$\delta\nu_{calc}$
$9_{27} \rightarrow 10_{28}$	$21/2 \rightarrow 23/2$	105265.42	105265.42	105265.50	0	+0.18
	$19/2 \rightarrow 21/2$				0	−0.01
	$17/2 \rightarrow 19/2$				0	−0.04
	$15/2 \rightarrow 17/2$				0	−0.22
$10_{29} \rightarrow 10_{28}$	$17/2 \rightarrow 17/2$	3178.92	3180.20	3180.40	−1.28	−1.23
	$23/2 \rightarrow 23/2$					−0.92
	$19/2 \rightarrow 19/2$	3181.45			−1.25	+0.89
	$21/2 \rightarrow 21/2$					+1.21

Table 1. Frequencies [MHz] ν_{obs} of $CD_3O^{35}Cl$ of Figs. 2 and 3. Unperturbed frequencies ν^0_{obs} and $\delta\nu_{obs}=\nu_{obs}-\nu^0_{obs}$ are compared with calculated ones, ν_{calc} and $\delta\nu_{calc}$, obtained by using parameters of Reference 18.

$\Delta K_- = 0$ transitions. Here we observed that HFS-transitions of a near prolate top can be pumped as a consequence of the near degeneracy of the $J_{K_-K_+}$ and $J_{K_-K'_+}$ levels. This is illustrated in Figure 6. On the right hand side the levels are drawn with an enlarged scale. $\Delta F = +1$ and $\Delta F = 0$ transitions are given by arrows, $\Delta F = -1$ transitions are not drawn. On the left side, the $J_{K_-K_+}$- and $J_{K_-K'_+}$-levels coincide. $\Delta F = \pm 1$ transition frequencies are not more distinguishable.

Figure 7a convinced us that it is hopeless to attempt an analysis of the contour of the band head recorded with Stark-modulation. As the analysis with the use of RF-MMW-double resonance is still quite complex it may help to consider the final result first. In Fig. 8 a Fortrat-diagram for the band head $J = 11 - 12$ is given. The intensity of the lines is marked by the length of the bars. The superposition of all these lines gives the contour of Figure 7a.

Working in operational mode I the pump frequencies of Table 2 were applied successively. The pump power was monitored at the second connector of the absorption cell and is given by the peak to peak voltage of the RF-bursts. Scanning the region of the band head by the signal frequency near 143,677 MHz the contour changes as shown in Figs. 7b – h left (l) and right (r). Only patterns involving pump transitions with $K_- \geqq 6$ are presented. The observed lines of Figs. 7b – h are given as dots in the two dimensional double resonance plot of Figure 9. It may be noticed that double resonance is observed also if the pump frequency nearly coincides with the pump transition (see p. e. Figs. 7cr and 7dr). By $\nu_p = 27.76$ MHz or 26.90 MHz the $J_{K_-} = 12_{11}$ and the $J_{K_-} = 11_{10}$ transitions are pumped. By application of 36.96 MHz for the $J_{K_-} = 11_{11}$- and 19.52 MHz for the $J_{K_-} = 12_{10}$-transitions (see Figs. 7br and 7dr) the assignment is made unambiguos. A closer inspection reveals that details are worked out that cannot be seen with Stark-modulation spectroscopy. Table 3 gives the observed frequency when transitions with $J = 11_{K_-}$ or $J = 12_{K_-}$ are pumped or when Stark modulation is used. In Table 4 by ν^0_{obs} the HFS unperturbed frequencies and the HFS-splittings $\delta\nu_{obs}$ are listed. The observed splittings are compared with calculated

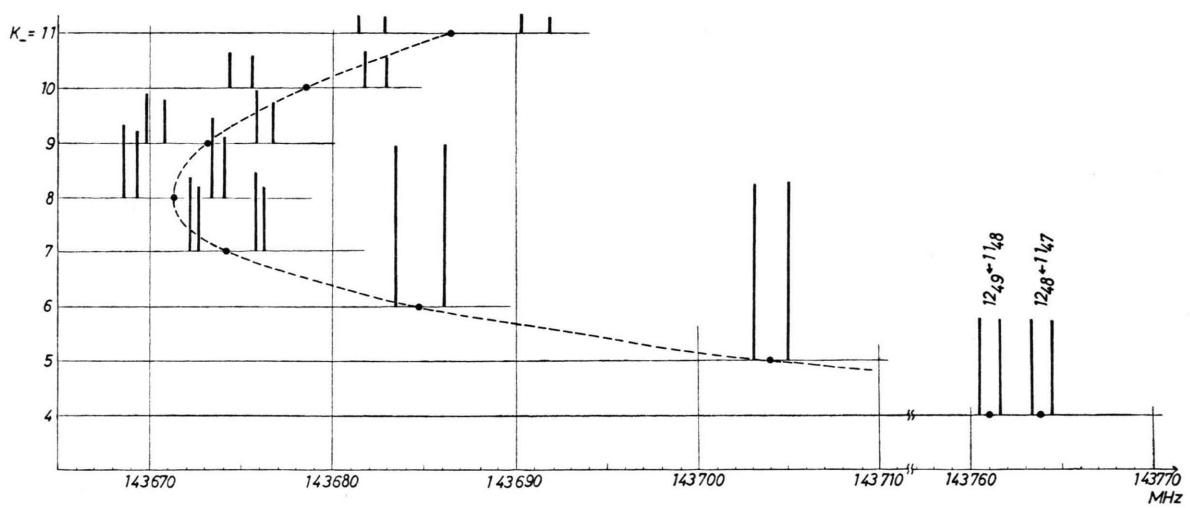

Fig. 8. Fortrat-diagram of the resolved $J = 11 \rightarrow 12$ band head of $CH_3O^{35}Cl$. The observed and unperturbed transition frequencies are given in Table 3 and 4. The intensity is marked by the length of the bars.

ones $\delta\nu_{\text{calc}}$, where the following rotational constants and quadrupole coupling constants were used[18]:

$A = 42064.286 \pm 0.011$ MHz,
$B = 6296.861 \pm 0.006$ MHz,
$C = 5670.610 \pm 0.005$ MHz,
$\chi_{aa}^{\text{Cl}} = 84.456 \pm 0.026$ MHz,
$\chi_{bb}^{\text{Cl}} = 25.361 \pm 0.022$ MHz,
$\chi_{cc}^{\text{Cl}} = 59.095$ MHz.

The consistancy of the data shows that the analysis of the band head was successful.

We think that RF-MMW double resonance is very useful as a selective modulation in the MMW-region

Table 2. Pump transitions $J_{K-K+} \rightarrow J_{K-K'+}$ mostly given as $J_{K-} \rightarrow J_{K-}$ ($\Delta K_+ = 1$), pump frequencies ν_p [MHz] and RF fields $V_{\text{peak-peak}}$ [V] used in the measurements of $J = 12 \rightarrow 11$ transitions of CH_3OCl. Not all pump transitions have been included in Figs. 7 and 9: The last column gives the part of Fig. 7, where the pump frequency was applied.

$J_{K-K+} \rightarrow J_{K-K'+}$	$F \rightarrow F'$	ν_p [MHz]	V [Volt] peak to peak	Figure
$12_{11} \rightarrow 12_{11}$	$27/2 \rightarrow 25/2$ $21/2 \rightarrow 23/2$	27.76	30	7 c r
	$23/2 \rightarrow 25/2$	3.38	25	
$11_{11} \rightarrow 11_{11}$	$25/2 \rightarrow 23/2$ $19/2 \rightarrow 21/2$	36.96	30	7 b r
	$21/2 \rightarrow 23/2$	4.86	25	7 h r
$12_{10} \rightarrow 12_{10}$	$27/2 \rightarrow 25/2$ $21/2 \rightarrow 23/2$	19.52	30	7 e r
$11_{10} \rightarrow 11_{10}$	$25/2 \rightarrow 23/2$ $19/2 \rightarrow 21/2$	26.90	30	7 d r
$12_9 \rightarrow 12_9$	$27/2 \rightarrow 25/2$ $21/2 \rightarrow 23/2$	11.80	30	7 c l
$11_9 \rightarrow 11_9$	$25/2 \rightarrow 23/2$ $19/2 \rightarrow 21/2$	17.79	30	7 b l
$12_8 \rightarrow 12_8$	$27/2 \rightarrow 25/2$ $21/2 \rightarrow 23/2$	4.93	20	7 e l
$11_8 \rightarrow 11_8$	$25/2 \rightarrow 23/2$ $19/2 \rightarrow 21/2$	9.64	30	7 d l
$12_7 \rightarrow 12_7$	$23/2 \rightarrow 21/2$ $25/2 \rightarrow 27/2$	1.14	10	7 g l
$11_7 \rightarrow 11_7$	$25/2 \rightarrow 23/2$ $19/2 \rightarrow 21/2$	2.46	20	7 f l
$12_6 \rightarrow 12_6$	$23/2 \rightarrow 21/2$ $25/2 \rightarrow 27/2$	6.39	25	7 f r
$11_6 \rightarrow 11_6$	$21/2 \rightarrow 19/2$ $23/2 \rightarrow 25/2$	3.75	18	7 g r
$12_5 \rightarrow 12_5$	$23/2 \rightarrow 21/2$ $25/2 \rightarrow 27/2$	10.82	24	
$11_5 \rightarrow 11_5$	$21/2 \rightarrow 19/2$ $23/2 \rightarrow 25/2$	9.00	30	
$11_{48} \rightarrow 11_{47}$	$19/2 \rightarrow 19/2$ $21/2 \rightarrow 21/2$ $23/2 \rightarrow 23/2$ $25/2 \rightarrow 25/2$	2.86	6	
$12_{49} \rightarrow 12_{48}$	$21/2 \rightarrow 21/2$ $23/2 \rightarrow 23/2$ $25/2 \rightarrow 25/2$ $27/2 \rightarrow 27/2$	5.75	6	
$11_{39} \rightarrow 11_{38}$	$19/2 \rightarrow 19/2$ $21/2 \rightarrow 21/2$ $23/2 \rightarrow 23/2$ $25/2 \rightarrow 25/2$	197.50	6	
$12_{310} \rightarrow 12_{39}$	$21/2 \rightarrow 21/2$ $23/2 \rightarrow 23/2$ $25/2 \rightarrow 25/2$ $27/2 \rightarrow 27/2$	328.56	1	

Table 4. Unperturbed transition frequencies ν^0_{obs} [MHz] of the HFS components $\bar{\nu}_{\text{obs}}$ of Table 3 and HFS splittings $\delta\nu_{\text{obs}} = \bar{\nu}_{\text{obs}} - \nu^0_{\text{obs}}$ of the $J = 12 \rightarrow 11$, $\Delta K_- = 0$ transitions of CH_3OCl. $\delta\nu_{\text{calc}}$ was obtained with the constants given in the text.

K_-	ν^0_{obs}	$F' \leftarrow F$	$\delta\nu_{\text{obs}}$	$\delta\nu_{\text{calc}}$
11	143686.45	$25/2 \leftarrow 23/2$	−5.08	−5.12
		$23/2 \leftarrow 21/2$	−3.62	−3.65
		$27/2 \leftarrow 25/2$	+3.76	+3.80
		$21/2 \leftarrow 19/2$	+5.23	+5.27
10	143678.55	$25/2 \leftarrow 23/2$	−4.23	−4.22
		$23/2 \leftarrow 21/2$	−3.00	−3.04
		$27/2 \leftarrow 25/2$	+3.14	+3.16
		$21/2 \leftarrow 19/2$	+4.30	+4.33
9	143673.21	$25/2 \leftarrow 23/2$	−3.42	−3.40
		$23/2 \leftarrow 21/2$	−2.47	−2.49
		$27/2 \leftarrow 25/2$	+2.57	+2.57
		$21/2 \leftarrow 19/2$	+3.46	+3.48
8	143671.27	$25/2 \leftarrow 23/2$	−2.69	−2.66
		$23/2 \leftarrow 21/2$	−2.00	−1.99
		$27/2 \leftarrow 25/2$	+2.05	+2.05
		$21/2 \leftarrow 19/2$	+2.76	+2.72
7	143674.15	$25/2 \leftarrow 23/2$	−2.00	−2.01
		$23/2 \leftarrow 21/2$	−1.56	−1.55
		$27/2 \leftarrow 25/2$	+1.59	+1.59
		$21/2 \leftarrow 19/2$	+2.04	+2.05
6	143684.69	$25/2 \leftarrow 23/2$ $23/2 \leftarrow 21/2$	−1.31	−1.45 −1.17
		$27/2 \leftarrow 25/2$ $21/2 \leftarrow 19/2$	+1.32	+1.19 +1.47
5	143708.94	$25/2 \leftarrow 23/2$ $23/2 \leftarrow 21/2$	−0.93	−0.97 −0.85
		$27/2 \leftarrow 25/2$ $21/2 \leftarrow 19/2$	+0.94	+0.85 +0.98
4 $(12_{49} \leftarrow 11_{48})$	143761.07	$23/2 \leftarrow 21/2$ $25/2 \leftarrow 23/2$	−0.56	−0.58
		$27/2 \leftarrow 25/2$ $21/2 \leftarrow 19/2$	+0.55	+0.57
4 $(12_{48} \leftarrow 11_{47})$	143763.85	$23/2 \leftarrow 21/2$ $25/2 \leftarrow 23/2$	−0.56	−0.58
		$27/2 \leftarrow 25/2$ $21/2 \leftarrow 19/2$	+0.55	+0.57
3 $(12_{3,10} \leftarrow 11_{39})$	143831.48	$23/2 \leftarrow 21/2$ $25/2 \leftarrow 23/2$	−0.34	−0.38 −0.28
		$21/2 \leftarrow 19/2$ $27/2 \leftarrow 25/2$	+0.32	+0.26 +0.35
3 $(12_{39} \leftarrow 11_{38})$	143962.31	$23/2 \leftarrow 21/2$ $25/2 \leftarrow 23/2$	−0.31	−0.36 −0.25
		$21/2 \leftarrow 19/2$ $27/2 \leftarrow 25/2$	+0.28	+0.23 +0.33

Table 3. Transition frequencies [MHz] of the $J=12\rightarrow 11$, $\Delta K_-=0$, $\Delta K_+=1$ transition of CH_3OCl. $\nu_{obs(i)}$, $i=1-3$ are obtained by pumping $J=11$- or $J=12$-transitions or using Stark-modulation. $\bar{\nu}_{obs}$ is the mean value. By K quantum numbers instead of frequencies it is indicated that overlapping of lines is present.

K_-	$F'\rightarrow F$	$\nu_{obs(1)}$	$\nu_{obs(2)}$	$\nu_{obs(3)}$	$\bar{\nu}_{obs}$
11 [a]	25/2 → 23/2	143681.37	(K=11) + (K=10)	(K=11) + (K=10)	143681.37
	23/2 → 21/2	143682.83	(K=11) + (K=10)	(K=11) + (K=10) + (K=6)	143682.83
	27/2 → 25/2	143690.22	143690.26	143690.14	143690.21
	21/2 → 19/2	143691.65	143691.69	143691.68	143691.68
10 [a]	25/2 → 23/2	143674.28	143674.36	(K=10) + (K=8)	143674.32
	23/2 → 21/2	143675.54	143675.55	(K=10) + (K=9) + K=7)	143675.55
	27/2 → 25/2	143681.70	143681.67	(K=11) + (K=10)	143681.69
	21/2 → 19/2	143682.83	143682.87	(K=11) + (K=10) + (K=6)	143682.85
9 [a]	25/2 → 23/2	143669.80	143669.82	143669.76	143669.79
	23/2 → 21/2	143670.75	143670.74	143670.72	143670.74
	27/2 → 25/2	143675.82	143675.74	(K=9) + (K=7)	143675.78
	21/2 → 19/2	143676.64	143676.70	(K=9) + (K=7)	143676.67
8 [a]	25/2 → 23/2	143668.58	143668.57	143668.60	143668.58
	23/2 → 21/2	143669.27	143669.26	143669.27	143669.27
	27/2 → 25/2	143673.38	143673.29	143673.29	143673.32
	21/2 → 19/2	143674.01	143674.04	(K=10) + (K=8)	143674.03
7 [a]	25/2 → 23/2	143672.01	143672.16	143672.29	143672.15
	23/2 → 21/2	143672.59	143672.66	143672.52	143672.59
	27/2 → 25/2	143675.73	143675.74	(K=10) + (K=9) + (K=7)	143675.74
	21/2 → 19/2	143676.17	143676.21	(K=9) + (K=7)	143676.19
6 [a]	25/2 → 23/2 23/2 → 21/2	143683.38	143683.38	(K=11) + (K=10) + (K=6)	143683.38
	27/2 → 25/2 21/2 → 19/2	143686.03	143686.01	143686.00	143686.01
5 [a]	25/2 → 23/2 23/2 → 21/2	143708.02	143708.03	143708.99	143708.01
	27/2 → 25/2 21/2 → 19/2	143709.87	143709.91	143709.85	143709.88
4 [a] ($12_{49}\rightarrow 11_{48}$)	23/2 → 21/2 25/2 → 23/2	143760.45	143760.57	143760.56 [d]	143760.51
	27/2 → 25/2 21/2 → 19/2	143761.57	143761.67	143761.64 [d]	143761.62
4 [b] ($12_{48}\rightarrow 11_{47}$)	23/2 → 21/2 25/2 → 23/2	143763.34	143763.23	143763.24 [d]	143763.29
	27/2 → 25/2 21/2 → 19/2	143764.43	143764.37	143764.31 [d]	143764.40
3 [c] ($12_{3,10}\rightarrow 11_{39}$)	23/2 → 21/2 25/2 → 23/2	143831.20	143831.08	143831.14 [d]	143831.14
	27/2 → 25/2 21/2 → 19/2	143831.85	143831.75	143831.80 [d]	143831.80
3 [c] ($12_{39}\rightarrow 11_{38}$)	23/2 → 21/2 25/2 → 23/2	143969.96	143962.03	143961.92 [d]	143962.00
	27/2 → 25/2 21/2 → 19/2	143962.53	143962.64	143962.53 [d]	143962.59

[a] $\Delta F=+1$ and $\Delta K_-=0$ transitions of the A- and E-levels were pumped. Pump frequencies are given in Table 2 and in Fig. 7 for $K\geqslant 6$.
[b] The $11_{47}\rightarrow 11_{48}$ and $12_{48}\rightarrow 12_{49}$ torsional A-transitions were pumped. See Table 2.
[c] The $11_{38}\rightarrow 11_{39}$ and $12_{3,10}\rightarrow 12_{39}$ transitions were pumped. See Table 2. Torsional A- and E-transitions not resolved.
[d] Observed by video detection.

and as a method for increasing the sensitivity in the region below 4000 MHz.

It may be an important help in analysing crowed spectra.

Acknowledgements

We thank Mr. M. Andolfatto for the preparation of the substances. The authors express their thanks to the members of the Kiel laboratory for many

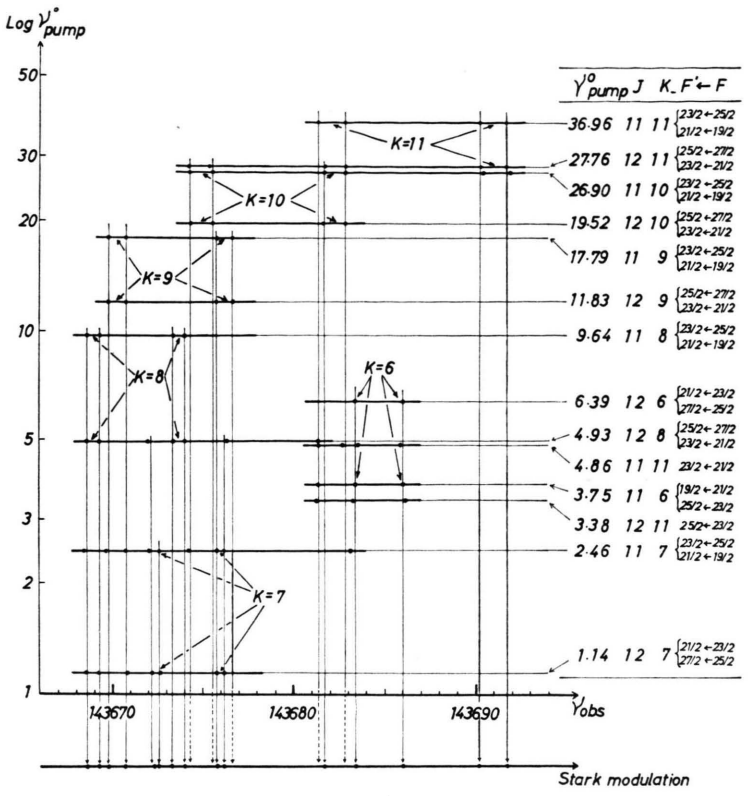

Fig. 9. Two dimensional double resonance plot of $\nu_p{}^0$ versus ν_{obs}. Pump frequencies $\nu_p{}^0$ and transitions are given in detail on the right hand side. Lines are indicated by dots. The superposition of the single HFS-patterns is indicated at the bottom. This corresponds the contour of the band head recorded with Stark modulation. Frequencies MHz.

helpful discussions. Further we thank the Deutsche Forschungsgemeinschaft and the Fonds der Chemie for a post-doctoral fellowship (M. S.) and for research funds. Calculations have been made with the PDP 10 and X8 of the Rechenzentrum der Universität Kiel.

[1] H. D. Rudolph, H. Dreizler, and U. Andresen, Z. Naturforsch. **26 a**, 233 [1971].
[2] U. Andresen and H. D. Rudolph, Z. Naturforsch. **26 a**, 320 [1971].
[3] R. Schwarz and H. Dreizler, Z. Naturforsch. **27 a**, 708 [1972].
[4] F. Scappini and A. Guarnieri, Z. Naturforsch. **27 a**, 1011 [1972].
[5] F. Scappini, A. Guarnieri, H. Dreizler, and P. Rademacher, Z. Naturforsch. **27 a**, 1329 [1972].
[6] R. Schwarz, H. Dreizler, and A. Guarnieri, Z. Naturforsch. **30 a**, 180 [1975].
[7] H. Mäder, H. Dreizler, and A. Guarnieri, Z. Naturforsch. **30 a**, 693 [1975].
[8] G. K. Pandey and H. Dreizler, Z. Naturforsch. **31 a**, 357 [1976].
[9] A. Di Giacomo, Nuovo Cim. **14**, 1082 [1952].
[10] A. Battaglia, A. Di Giacomo, and S. Santuccio, Nuovo Cim. **43 B**, 89 [1966].
[11] A. P. Cox, W. G. Flynn, and E. B. Wilson jr., J. Chem. Phys. **42**, 3094 [1965].
[12] R. C. Woods III, A. M. Ronn, and E. B. Wilson jr., Rev. Sci. Instrum. **37**, 927 [1966].
[13] O. L. Stiefvater, Z. Naturforsch. **30 a**, 1765 [1975].
[14] P. G. Favero, F. Scappini, and A. M. Mirri, Boll. Sci. Fac. Chim. Ind. **24**, 93 [1966].
[15] S. H. Autler and C. H. Townes, Phys. Rev. **100**, 703 [1955].
[16] F. J. Wodarczyk and E. B. Wilson jr., J. Mol. Spectr. **37**, 445 [1971].
[17] J. L. Destombes and C. Marlière, Priv. Communication of Prof. Wertheimer, Lille.
[18] M. Suzuki and A. Guarnieri, to be published.